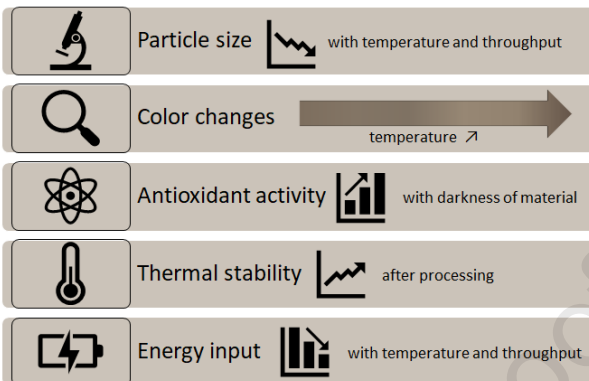




Extrusion grinding

Temperature

Shear forces



Journal Pre-proof

1 **Sustainable upcycling of brewers' spent grain by thermo-mechanical treatment in twin-** 2 **screw extruder**

4 **Abstract**

5 Thermo-mechanical treatment of brewers' spent grain (a by-product of beer manufacturing)
6 was successfully performed via the extrusion process. The impact of temperature (from 30 to
7 180 °C), throughput (from 1 to 5 kg/h) and screw speed (from 75 to 375 rpm) on particle size,
8 color, chemical structure, antioxidant activity and thermal stability of resulting material, as
9 well as correlations between particular properties, were investigated. The color of treated
10 brewers' spent grain was strongly influenced by particle size and the extent of Maillard
11 reactions occurring during extrusion, responsible for the browning of material. Moreover,
12 products of these reactions, melanoidins, enhanced the antioxidant activity of brewers' spent
13 grain, which after extrusion at 180 °C was increased by even 100%. Thermo-mechanical
14 treatment of brewers' spent grain at 120 and 180 °C increased its thermal stability
15 investigated by thermogravimetric analysis. It was also observed that temperature treatment
16 above 100 °C also led to the reduction in friction inside the extruder barrel and reduced by at
17 least 20% specific mechanical energy required to brewers' spent grain modification, which
18 positively affects the economic aspect of the process. The results confirm that a proper
19 adjustment of extrusion parameters allows easy tailoring of the appearance (color, particle
20 size distribution) and performance properties (thermal stability, antioxidant activity) of
21 brewers' spent grain, which significantly extend applications of this cellulosic-rich waste in
22 wood polymer composites technology.

23 **Keywords**

24 Brewers' spent grain; upcycling; thermo-mechanical treatment; extrusion; color and
25 performance properties; chemical structure



26 1. Introduction

27 Wood polymer composites (WPCs) are a class of composites consisting of one or
28 more lignocellulosic fillers and one or a mixture of polymeric materials. Thanks to the
29 application of lignocellulosic fillers, these materials may be characterized, e.g., with lower
30 density, higher stiffness, renewable nature, biodegradability, and reduced costs (Zajchowski
31 and Ryszkowska, 2009). Moreover, due to lower hardness, the application of lignocellulosic
32 filler reduces machine wear and damage of processing equipment comparing to, e.g., mineral
33 fillers, commonly used in polymer composites.

34 In order to obtain WPCs with desired parameters, used fillers need to show particular
35 properties. Fillers' properties affect the performance of the resulting WPCs. However, one of
36 the most important is the particle size distribution. It was repeatedly proven that smaller
37 particles often show higher specific surface areas, which together enhance the mechanical
38 performance of composites (Fu et al., 2008). Moreover, the small particle size of filler may
39 enhance the barrier properties of the composite, which can have an influence on, e.g., the rate
40 of biodegradation (Kargarzadeh et al., 2017, 2018). Currently applied methods of size
41 reduction of fillers are mostly based on processes with periodic character and use of various
42 types of mills (Bridgeman et al., 2007; Silva et al., 2011). More perspective solutions, which
43 are more cost-effective, should be based on continuous processes, such as extrusion, which
44 was applied in the presented study.

45 Another parameter, essential for the applications of WPCs, affecting their aesthetic
46 aspect is their color. Commonly used natural fillers may vary in color because of different
47 type and source of raw material (e.g., different types of wood or other lignocellulosic fillers),
48 but also because of the applied treatment, most often associated with size reduction. During
49 grinding or milling of fillers, shear forces and sometimes also the temperature is applied to the
50 material, which is inducing color changes of material.



51 Generally, changes in color during grinding of fillers are associated with two factors:
52 final particle size and chemical reactions occurring inside the material during processing. The
53 changes in the roughness of the surface, hence light scattering and particle size of fillers,
54 significantly affect the light transmittance, which was confirmed for diverse natural materials
55 (Bolade et al., 2009; Sun et al., 2016).

56 Chemical reactions resulting in the changes in color are generally referred to as non-
57 enzymatic browning reactions. This group consists mainly of caramelization and Maillard
58 reactions. The first reaction is a complex process of sugar pyrolysis, including, e.g.,
59 dehydration, condensation, fragmentation, isomerization, or polymerization reactions of
60 sugars, resulting in the generation of caramelans ($C_{24}H_{36}O_{18}$), caramelens ($C_{36}H_{50}O_{25}$) and
61 caramelins ($C_{125}H_{188}O_{80}$) (Villamiel et al., 2006). During caramelization, volatile compounds
62 are also formed, which are responsible for characteristic caramel flavor. Maillard reactions,
63 which involve chemical reactions between amino groups of amino acids and carbonyl groups
64 of sugars, can take place at lower temperatures than caramelization. They involve reactions of
65 reducing sugars with amino acids and result in the hard to characterize complex mixture of
66 compounds responsible for the final color and flavor of resulting material, which is very
67 important in polysaccharide-based food products, such as cookies, biscuits, bread, etc.
68 (Maillard, 1912). Generally, a group of resulting products, responsible for the color change, is
69 referred to as melanoidins – higher molecular weight oligomeric and polymeric substances
70 (Martins et al., 2000). The general scheme of Maillard reactions, which show their
71 complexity, is presented in Fig. S1. It is also crucial that melanoidins are commonly known in
72 food chemistry and technology for their antioxidant activity, which enhances the storage
73 stability of various food products (Pastoriza and Rufián-Henares, 2014; Rivero-Pérez et al.,
74 2002). Therefore, based on the literature data, it can be assumed that they could also enhance
75 the stability of WPCs (Moraczewski et al., 2019).



76 From an economical and ecological point of view, the most beneficial is the
77 incorporation of fillers, which are considered as by-products or wastes resulting from the
78 processing of renewable raw materials. Therefore, it seems very interesting for the
79 manufacturing of polymer biocomposites to use the brewers' spent grain (BSG), which is the
80 major by-product of the brewing industry, generated in the mashing process (Hejna et al.,
81 2015). BSG shows relatively similar composition to various waste fillers applied during the
82 preparation of WPCs, e.g., pulp resulting from the paper industry or wood flour. However, it
83 contains significantly higher amounts of proteins, which can participate in Maillard reactions,
84 enhancing the antioxidant activity of filler (Rufián-Henares and Morales, 2007). BSG stands
85 for ~85% of the total by-products of beer manufacturing, and according to literature data,
86 accounts for around 31% of the initial malt weight (Mussatto et al., 2006). According to The
87 Brewers of Europe Beer Statistics Report from 2018 (The Brewers of Europe, 2018),
88 European producers manufacture over 41 billion liters of beer each year, which results in the
89 generation of over 2.5 million tonnes of BSG. Market Research Store reports that global
90 production of WPCs is increasingly growing, from almost 3.5 million tonnes in 2015 to over
91 4.3 million tonnes in 2017, and is expected to reach over 6.0 million tonnes in 2020 (Market
92 Research Store, 2018). Therefore, research associated with the development of this group of
93 materials is very perspective. Assuming with average filler share of 50 wt.% in WPCs, the
94 current demand on lignocellulosic fillers is around 2.2 million tonnes annually, so it can be
95 seen that utilization of BSG produced only in Poland could be a significant contribution to
96 WPCs market.

97 The main limitation related to the application of BSG in polymer composites is related
98 to two factors: relatively high humidity and large particle size of this cellulosic-rich waste.
99 The dried form of BSG is present in the market. Therefore this research work is focused on
100 solving the issues related to the particle size of BSG and the characteristics of ground BSG.



101 So far, BSG has not been very often investigated as a filler for WPCs. In previous
102 works, BSG was successfully applied as filler into rigid polyurethane foams (Formela et al.,
103 2017; Hejna et al., 2017), natural rubber (Zedler et al., 2018, 2020), and poly(ϵ -caprolactone)
104 (Hejna et al., 2015). Obtained results indicated that proteins present in BSG acted as
105 plasticizers and reduced the adhesion to polymer matrices. Therefore, suitable treatment of
106 BSG prior application in WPCs should be investigated in order to understand how the
107 changes in the chemical structure of BSG affect their impact on compatibility with polymer
108 matrices. Authors investigating polymer/BSG composites (Berthet et al., 2015; Cunha et al.,
109 2014; Revert et al., 2017) studied the microscopic structure, mechanical, and thermal
110 properties of obtained WPCs, which indicated insufficient interfacial adhesion between matrix
111 and filler. The only modification of filler was alkali treatment applied by Berthet et al. (2015).
112 However, they were not able to prepare WPCs due to the aggregation of the fibers. Therefore,
113 the effect of treatment could not be evaluated. Moreover, the impact of melanoidins,
114 potentially enhancing the resistance of composites towards oxidation, has not been
115 investigated yet.

116 In this paper, sustainable upcycling of brewers` spent grain by thermo-mechanical
117 treatment in the twin-screw extruder was developed. The twin-screw extruder was selected
118 due to: i) high mixing and shearing efficiency of processed material; ii) common application
119 in the industry (more straightforward implementation of laboratory results at industrial scale),
120 and iii) continuity of process (high throughput and good repeatability of results). Recently,
121 extrusion techniques found application in the treatment of biomass and lignocellulosic wastes
122 (Duque et al., 2017; Leonard et al., 2019; Offiah et al., 2018). However, there is a lack of
123 published information about the application of this technique for utilization or up-cycling of
124 brewers` spent grain. Therefore, in this research work, the impact of extrusion conditions
125 (temperature, throughput, screw speed) on the specific mechanical energy required to BSG



126 particles size reduction, particle size distribution, chemical structure, color properties, thermal
127 stability and antioxidant activity of treated BSG were investigated in order to evaluate the
128 possibility of its application in wood polymer composites technology.

129

130 2. Experimental

131 2.1. Materials

132 Brewers' spent grain used in the presented study was obtained from Energetyka
133 Złoczew sp. z o.o. (Poland). It was waste from the production of light lager and consisted
134 solely of barley malts. The supplier already dried obtained BSG. In Fig. 1, there is shown the
135 appearance of used BSG.

136 Synthetic 2,2-diphenyl-1-picrylhydrazyl (DPPH) radical ($\geq 95\%$, solid crystal) and
137 70% water solution of ethanol were used during the determination of the antioxidant activity
138 of modified BSG. Both compounds were acquired from Sigma Aldrich (Poland) and used as
139 received.



140

141 **Figure 1.** Macroscopic (a) and microscopic (b) appearance of applied BSG before extrusion grinding.

142

143

144

145 2.2. Extrusion grinding of BSG

146 Extrusion grinding of BSG was performed with EHP 2x20 Sline co-rotating twin-
147 screw extruder from Zamak Mercator (Poland), following patent application (Hejna and
148 Formela, 2019). The extruder has eleven heating/cooling zones with a screw diameter of 20
149 mm and an L/d ratio of 40. The screw configuration is shown in Fig. S2. BSG was dosed into
150 the extruder by a volumetric feeder with a constant throughput of 1, 3, or 5 kg/h. Screw speed
151 varied from 75 to 225, from 150 to 300 and from 225 to 375 rpm, respectively, for increasing
152 throughput. Barrel temperature in all zones was set at 30, 60, 120, or 180 °C. For each set of
153 parameters, extrusion was carried out for at least 60 minutes after stabilization of the motor
154 load of the extruder, which indicated stabilization of the process. After grinding, samples of
155 BSG were left in order to cool down to room temperature. Samples were coded as X/Y/Z,
156 where X stands for the processing temperature, Y for the throughput, and Z for the screw
157 speed.

158

159 2.3. Characterization techniques

160 The characterization of the particle size distribution of investigated BSG fillers was
161 evaluated using a laser particle sizer Fritsch ANALYSETTE 22 apparatus operated in the
162 range of 0.08 - 2000 µm.

163 The chemical structure of studied samples was determined using Fourier transform
164 infrared spectroscopy (FTIR) analysis performed by a Nicolet Spectrometer IR200 from
165 Thermo Scientific (USA). The device had an ATR attachment with a diamond crystal.
166 Measurements were performed with 1 cm⁻¹ resolution in the range from 4000 to 400 cm⁻¹ and
167 64 scans. For each sample, at least three spectra were recorded.



168 The color of treated BSG was evaluated according to the Commission Internationale
 169 de l'Eclairage (CIE) through $L^*a^*b^*$ coordinates (International Commission on Illumination,
 170 1978). In this system, L^* is the color lightness ($L^*=0$ for black and $L^*=100$ for white), a^* is
 171 the green(-) / red(+) axis, and b^* is the blue(-) / yellow(+) axis. Thirty tests of each sample
 172 were done and used for the determination of arithmetic mean values. The color was
 173 determined by optical spectroscopy using HunterLab Miniscan MS/S-4000S
 174 spectrophotometer, placed additionally in a specially designed light trap chamber. The total
 175 color difference parameter (ΔE^*) was calculated according to the following formulation (1)
 176 (Bociaga and Trzaskalska, 2016):

$$177 \quad \Delta E^* = [(\Delta L^*)^2 + (\Delta a^*)^2 + (\Delta b^*)^2]^{0.5} \quad (1)$$

178 Moreover, obtained values of a^* and b^* may be used to calculate other parameters
 179 used to describe colors, such as chroma and hue, defined by the following equations (2 and 3):

$$180 \quad C_{ab}^* = (a^{*2} + b^{*2})^{\frac{1}{2}} \quad (2)$$

$$181 \quad h_{ab} = \tan^{-1} \left(\frac{b^*}{a^*} \right) \quad (3)$$

182 Determined color parameters were also converted to the commonly used Adobe RGB
 183 color space defined by the three chromaticities of the red, green, and blue additive primaries
 184 (Hunt, 2004). The first step was the conversion from CIELab to normalized CIEXYZ space
 185 according to the following equations (4-8) (Lopez et al., 2005):

$$186 \quad X = X_w f^{-1} \left(\frac{L^*+16}{116} + \frac{a^*}{500} \right) \quad (4)$$

$$187 \quad Y = Y_w f^{-1} \left(\frac{L^*+16}{116} \right) \quad (5)$$

$$188 \quad Z = Z_w f^{-1} \left(\frac{L^*+16}{116} - \frac{b^*}{200} \right) \quad (6)$$

189 where:

$$190 \quad f^{-1}(t) = \begin{cases} t^3 & t > \delta \\ 3\delta^2 \left(t - \frac{4}{29} \right) & \text{otherwise} \end{cases} \quad (7)$$

191 and

$$192 \quad \delta = \frac{6}{29} \quad (8)$$

193 and

194 X_w , Y_w and Z_w are the values for the reference white point, which for Illuminant D65 equal
195 0.950450, 1.000000 and 1.088754, respectively, according to ITU-R Recommendation
196 BT.709.

197 Next, conversion from CIEXYZ color space to linear RGB (v) was made according to
198 the following formulas (9-20):

$$199 \quad \begin{bmatrix} r \\ g \\ b \end{bmatrix} = [M]^{-1} \begin{bmatrix} X \\ Y \\ Z \end{bmatrix} \quad (9)$$

200 where:

$$201 \quad [M] = \begin{bmatrix} S_r X_r & S_g X_g & S_b X_b \\ S_r Y_r & S_g Y_g & S_b Y_b \\ S_r Z_r & S_g Z_g & S_b Z_b \end{bmatrix} \quad (10)$$

202 where:

$$203 \quad X_r = \frac{x_r}{y_r} \quad (11)$$

$$204 \quad Y_r = 1 \quad (12)$$

$$205 \quad Z_r = \frac{(1-x_r-y_r)}{y_r} \quad (13)$$

$$206 \quad X_g = \frac{x_g}{y_g} \quad (14)$$

$$207 \quad Y_g = 1 \quad (15)$$

$$208 \quad Z_g = \frac{(1-x_g-y_g)}{y_g} \quad (16)$$

$$209 \quad X_b = \frac{x_b}{y_b} \quad (17)$$

$$210 \quad Y_b = 1 \quad (18)$$

211
$$Z_b = \frac{(1-x_b-y_b)}{y_b} \quad (19)$$

212
$$\begin{bmatrix} S_r \\ S_g \\ S_b \end{bmatrix} = \begin{bmatrix} X_r & X_g & X_b \\ Y_r & Y_g & Y_b \\ Z_r & Z_g & Z_b \end{bmatrix}^{-1} \begin{bmatrix} X_w \\ Y_w \\ Z_w \end{bmatrix} \quad (20)$$

213 and:

214 (x_r, y_r) , (x_g, y_g) , and (x_b, y_b) are chromaticity coordinates of RGB system, which in the case of
215 Adobe RGB are (0.64, 0.33), (0.21, 0.71) and (0.15, 0.06), while X_w , Y_w and Z_w are the values
216 for the reference white point, as mentioned above (Adobe Systems Incorporated, 2005).

217 Conversion from linear RGB (v) to nonlinear RGB (V) was made using gamma
218 companding according to the following equation (21):

219
$$V = v^{\frac{1}{\gamma}} \quad (21)$$

220 where γ stands for gamma value characteristic for a color system, in the case of Adobe RGB
221 equals 2.2.

222 Obtained RGB values were in the nominal range [0.0, 1.0]. In order to present them in
223 the most commonly used range of [0, 255], components were multiplied by 255.

224 Samples of extruded BSG for the determination of antioxidant activity were prepared
225 by the extraction of proper compounds in the following manner. Samples with a mass of 1 g
226 were weighed on analytical balance with an accuracy of 0.001 g and then mixed with 9 cm³ of
227 70% solution of ethanol. The mixtures were shaken vigorously and allowed to stand at room
228 temperature in the dark for 20 hours. All extracts were centrifuged in a centrifuge Hettich
229 Rotina 380 for 3 minutes at 3500 rpm. Subsequently, the antioxidant activity of supernatants
230 was determined with a modified method described by Brand-Williams et al. (1995) using
231 synthetic DPPH radical – 2,2-diphenyl-1-picrylhydrazyl. Three specimens were analyzed for
232 each sample. For each analysis, 1 ml of analyzed extract was mixed with 5 ml of the 0.5 mM
233 DPPH solution. The absorbance of the mixtures (A_i) was measured at 517 nm after 15

234 minutes of incubation at room temperature. The negative control (A_0) was prepared for 1 ml
235 of 70% ethanol. The percent DPPH scavenging effect was calculated by using the following
236 equation (22):

$$237 \quad I_{\%} = \frac{(A_0 - A_i)}{A_0} \cdot 100\% \quad (22)$$

238 The thermal analysis was performed using the TG 209 F3 apparatus from Netzsch
239 (Germany). Samples of composites weighing approx. 10 mg were placed in a ceramic dish.
240 The study was conducted in an inert gas atmosphere - nitrogen in the range from 30 to 900 °C
241 with a temperature increase rate of 10 °C/min. Two specimens were analyzed for each sample.

242 In order to evaluate the effect of barrel temperature on the progress of ground tire
243 rubber reclamation, the specific mechanical energy (SME, in kWh/kg) was determined. SME
244 was calculated using equation (23):

$$245 \quad SME = \frac{N}{Q} \quad (23)$$

246 where N is the consumption of drive motor power (kW), and Q is throughput (kg/h). For
247 calculations of the specific mechanical energy, the average motor load from at least 60
248 minutes of extrusion was used.

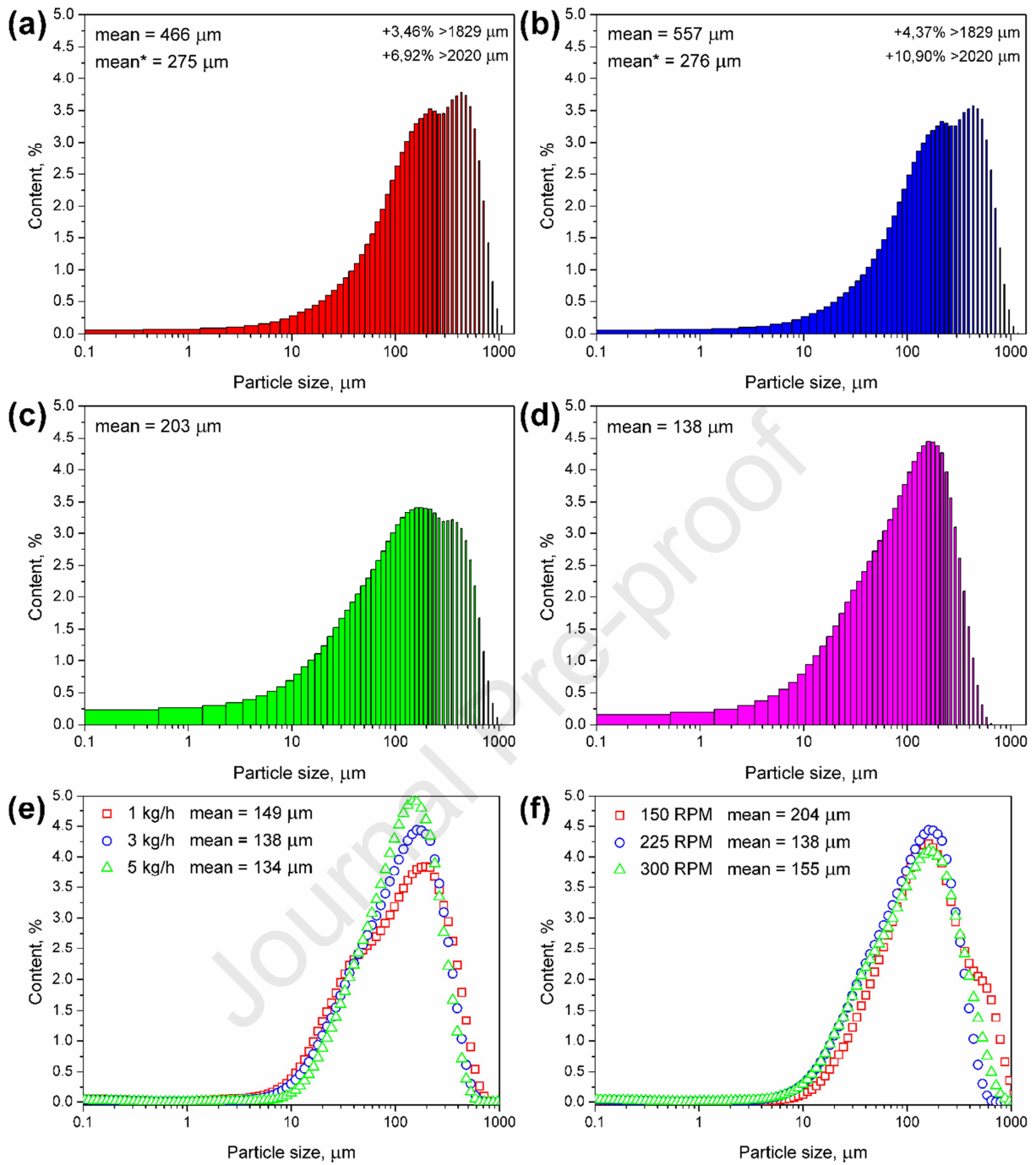
249

250 **3. Results and discussion**

251 *3.1. Particle size distribution*

252 Fig. 2 shows the particle size distribution of the selected filler samples in order to
253 determine its dependence on the adjusted extrusion parameters. The impact of process
254 temperature on the particle size of obtained samples (for throughput of 3 kg/h and a screw
255 speed of 225 rpm) is presented in Fig. 2a-d. It can be seen that lower extrusion temperatures,
256 below 100 °C, resulted in larger particle sizes, due to the agglomeration of treated BSG

257 related to higher moisture content. At lower temperatures (30 and 60 °C), moisture present in
258 the BSG due to its hygroscopic nature (as other lignocellulosic materials) combined with the
259 external forces causes granulation of particles. Such an effect is related to the enhanced
260 hydrogen bonding between lignocellulosic particles caused by the presence of moisture
261 (Sahputra et al., 2019). As a result, particles bigger than 1200 µm were present in extruded
262 material, which is presented in Fig. 2a and 2b. Such an effect is often observed during
263 extrusion cooking and used in the manufacturing of grain flakes and snacks (Dhanalakshmi et
264 al., 2011). The appearance of these particles is presented in Fig. S3. The increase of the
265 process temperature to 120 °C resulted in the reduction of average particle size, which is
266 related to the lower share of particles bigger than 300 µm, and lack of agglomerates.
267 Nevertheless, only for the temperature of 180 °C distribution of particle, diameters were
268 noticeably more homogenous, comparing to lower temperatures. Such an effect was probably
269 associated with the lower moisture content and partial decomposition of the extractives and
270 other low molecular weight components of BSG (Mahmood et al., 2013).



271

272

273

274 **Figure 2.** The particle size distribution of samples extruded with a screw speed of 225 rpm and throughput of 3
 275 kg/h at (a) 30 °C, (b) 60 °C, (c) 120 °C and (d) 180 °C, as well as the impact of (e) throughput and (f) screw
 276 speed on particle size distribution.

277

278 Fig. 2e shown the impact of the extrusion throughput on the particle size distribution
 279 of ground BSG (for process temperature of 180 °C and a screw speed of 225 rpm).
 280 Throughput is associated with the degree of fill of extruder barrel, hence the level of shear

281 forces between the BSG particles and between particles and extruder barrel (Kao and Allison,
282 1984). Suparno et al. (2010) developed a model based on experimental data, which indicates
283 that shear forces are significantly increasing with the degree of fill of extruder barrel.
284 However, an increase in throughput shows the opposite effect because it is associated with
285 shorter residence time in the extruder and its more homogenous distribution (Altomare and
286 Ghossi, 1986). In the presented case, it resulted in noticeably more homogenous particle size
287 distribution and slightly smaller average particle size (Yeh et al., 1992). Such effect may be
288 considered very beneficial from the potential application point of view (e.g., in wood polymer
289 composites) because it enables the preparation of material showing superior properties with
290 higher efficiency.

291 The plot in Fig. 2f presents the impact of screw speed on the particle size distribution
292 of BSG ground at 180 °C and with a throughput of 3 kg/h. It can be seen that despite the
293 similar distribution of particle size, differences between screw speed of 150 rpm and higher
294 values were noted. Such an effect is associated with the increase of shear forces inside the
295 extrusion barrel for higher screw speed values, which facilitate the disintegration of BSG
296 particles. A similar effect was observed for the extrusion treatment of ground tire rubber
297 particles by Formela et al. (2014). On the other hand, similar to throughput, an increase of
298 screw speed shows opposite effects associated with the shortening of material's residence
299 time in the extruder barrel. As a result, the increase of screw speed over 225 rpm for analyzed
300 process parameters increased average particle size.

301

302 *3.2. Color properties*

303 The color parameters of prepared BSG samples are presented in Table 1. As mentioned
304 above, in section 2.3. Measurements, the color of materials was evaluated using CIELab color
305 space, and then parameters were converted to popular Adobe RGB space. Moreover, the total



306 color difference parameter (ΔE^*) related to the unprocessed reference sample is presented, as
307 well as the color of obtained materials.

Journal Pre-proof

308 **Table 1.** Color parameters of extruded BSG samples and antioxidant activity of selected samples.

Temperature, °C	Throughput, kg/h	Screw speed, rpm	Color parameters							Antioxidant activity towards DPPH, %			
			L*	a*	b*	ΔE^*	R	G	B	Color	C _{ab} *	h _{ab} , °	
		Reference sample	48.17	5.11	13.04	-	124.8	110.3	93.8		14.0	68.6	36
		75	49.87	4.66	12.14	1.97	128.3	114.6	99.1		13.0	69.0	-
	1	150	56.50	4.71	13.43	8.35	145.8	130.9	112.8		14.2	70.7	-
		225	56.81	4.88	13.91	8.69	147.0	131.6	112.8		14.7	70.7	-
		150	51.98	4.87	13.09	3.82	134.2	119.6	102.6		14.0	69.6	-
30	3	225	50.97	4.61	12.31	2.94	131.1	117.3	101.4		13.1	69.5	49
		300	52.55	4.73	13.21	4.40	135.6	121.1	103.7		14.0	70.3	-
		225	50.37	4.80	12.45	2.30	129.8	115.8	99.8		13.3	68.9	-
	5	300	50.95	4.61	12.42	2.89	131.1	117.3	101.2		13.3	69.6	-
		375	53.44	5.03	13.70	5.32	138.3	123.1	105.1		14.6	69.8	-
		75	50.64	4.44	12.23	2.68	130.0	116.6	100.7		13.0	70.0	-
	1	150	51.50	4.70	13.27	3.36	132.9	118.5	101.2		14.1	70.5	-
		225	52.89	4.65	13.50	4.76	136.5	122.0	104.1		14.3	71.0	-
		150	50.18	4.81	12.60	2.08	129.4	115.3	99.1		13.5	69.1	-
60	3	225	49.60	4.60	11.83	1.94	127.4	114.0	98.9		12.7	68.8	49
		300	50.02	4.32	12.38	2.11	128.4	115.2	99.1		13.1	70.8	-
		225	50.41	4.69	12.59	2.32	129.9	115.9	99.7		13.4	69.6	-
	5	300	50.48	4.76	13.23	2.34	130.3	116.0	98.8		14.1	70.2	-
		375	51.35	4.84	12.67	3.21	132.4	118.1	101.7		13.6	69.1	-
		75	57.64	5.32	14.52	9.59	149.9	133.4	113.8		15.5	69.9	-
	1	150	58.23	4.92	14.35	10.15	150.9	135.1	115.5		15.2	71.1	54
		225	56.55	5.15	14.33	8.48	146.8	130.7	111.5		15.2	70.2	-
120		150	55.55	5.88	14.82	7.63	145.1	127.8	108.3		15.9	68.4	-
	3	225	56.29	5.42	14.14	8.20	146.3	129.9	111.2		15.1	69.0	54
		300	57.28	5.23	14.32	9.20	148.7	132.5	113.3		15.3	69.9	-

		225	57.15	5.50	14.46	9.10	148.7	132.0	112.8		15.5	69.2	-
	5	300	55.63	5.47	14.34	7.58	144.7	128.2	109.3		15.4	69.1	-
		375	56.32	5.42	14.29	8.25	146.4	130.0	111.0		15.3	69.2	-
		75	45.26	7.91	15.18	4.57	121.1	101.7	84.0		17.1	62.5	-
	1	150	49.33	7.15	15.33	3.28	130.6	111.8	93.0		16.9	65.0	-
		225	50.30	6.82	15.34	3.57	132.8	114.3	95.2		16.8	66.0	63
		150	37.38	7.29	12.02	11.05	100.4	84.1	71.3		14.1	58.8	73
180	3	225	47.23	7.68	15.23	3.50	125.8	106.4	88.3		17.1	63.2	71
		300	49.74	7.18	15.42	3.53	131.7	112.7	93.8		17.0	65.0	71
		225	42.43	7.57	13.59	6.27	113.3	95.3	80.0		15.6	60.9	-
	5	300	49.06	6.97	14.74	2.67	129.6	111.3	93.3		16.3	64.7	75
		375	48.46	7.31	15.28	3.15	128.6	109.6	91.1		16.9	64.4	-

309

310

311

312

313

314

315

316

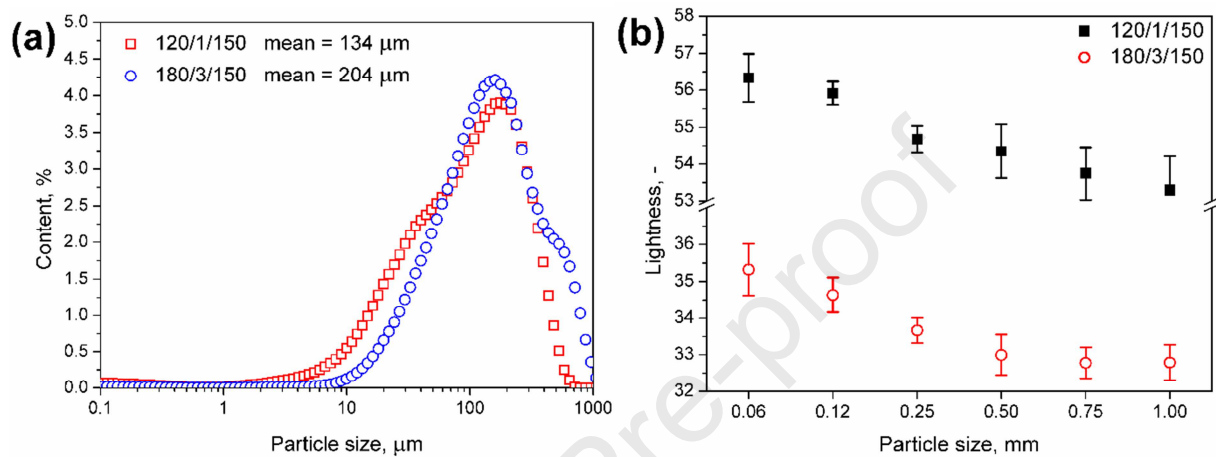
317 As mentioned above, CIELab color space defines color with three parameters, L^* , a^* ,
318 and b^* . According to equation (1), these parameters can be used to calculate the difference
319 between the color of particular materials. According to standard ISO 2813:2001, the value of
320 ΔE^* is associated with the human ability to distinguish colors and notice the color difference
321 (Bociaga and Trzaskalska, 2016).

322 Although all of them are affected by the physical structure of the material, the one
323 most significantly affected by the particle size is lightness (Ahmed et al., 2014, 2015, 2016).
324 Generally, independently of a^* and b^* parameters, hence hue of material, smaller particles
325 show higher lightness, which is associated with the increase of specific surface area that
326 allows more reflection of light (Chen et al., 1999; Horvath and Halasz-Fekete, 2005). In Table
327 S1, there are summarized results published by other researchers, which confirm the presented
328 results.

329 A similar phenomenon can be observed in the presented study. Most of the materials
330 prepared at lower temperatures (30 and 60 °C) had the highest values of average particle size
331 among analyzed samples. As a result, they were characterized by similar color properties to
332 the neat BSG. It was expressed by the values of ΔE^* parameter lower than 3.5, which indicate
333 invisible ($\Delta E^* < 1.0$), small (ΔE^* in the range of 1.0-2.0), or medium (ΔE^* in the range of 2.0-
334 3.5) color variations (Bociaga and Trzaskalska, 2016). Higher values, hence more significant
335 color variations, were noted for samples extruded with higher screw speed, which reduced
336 particle size and increased lightness of materials. Samples extruded at 120 °C show higher
337 lightness comparing to lower extrusion temperatures, as a result of smaller particle size.
338 Samples prepared at 180 °C were darker because of the chemical reactions occurring in the
339 material and possible partial decomposition of polysaccharides present in BSG. Nevertheless,
340 in Fig. 3, there is shown particle size distribution for the samples with the highest (120/1/150)
341 and the lowest (180/3/150) lightness. It can be seen that except chemical reactions also



342 particle size and its distribution shows a noticeable impact on the lightness of the material.
 343 Despite the better homogeneity of distribution for sample 180/3/150, the share of particles
 344 with lower diameters was higher for 120/1/150 samples. Hence its average particle size was
 345 lower. As a result, noticeable differences in lightness were observed, which, among other
 346 factors, was caused by different particle size distribution.



347 **Figure 3.** Particle size distribution for (a) samples with the lowest and the highest lightness and (b) fractions of
 348 these samples with various particle sizes.
 349

350 For more detailed analysis, the samples mentioned above were fractionated using
 351 sieves with diameters of 0.06, 0.12, 0.25, 0.50, 0.75, and 1.00 mm, and their color parameters
 352 were determined. The obtained results are presented in Fig. 3b and confirm results published
 353 by other researchers (Kim and Shin, 2014; Liu, 2009).

354 As mentioned above, two groups of reactions are responsible for color changes in
 355 treated BSG: caramelization and Maillard reactions. In the presented case, caramelization
 356 does not play a significant role because it involves mono- and disaccharides, which are hardly
 357 present in brewers' spent grain (they are removed during mashing) and occurs at temperatures
 358 of 160 °C or higher, except fructose (110 °C) (Mussatto et al., 2006). Only minimal amounts
 359 of lower molecular weight saccharides may be generated during extrusion due to the shear-
 360 induced breakdown of glycosidic links (Ott, 1964). Therefore, for the investigated materials,
 361 caramelization reactions were not so significant, especially when processing temperatures of

362 30 and 60°C were applied. More critical are Maillard reactions, because they can take place at
363 lower temperatures than caramelization. They involve reactions of reducing sugars, which can
364 be present in BSG in the amount of ~15 wt.% (Waters et al., 2012). Except for typical
365 reducing sugars, also other BSG compounds, lignin may show some reducing potential due to
366 the presence of aldehyde groups, hence the ability to take part in Maillard reactions (Maillard,
367 1912). Moreover, BSG usually contains at least 15-20 wt.% of proteins, among which the
368 most popular amino acids, which take part in Maillard reactions, are histidine, glutamic acid,
369 lysine, and leucine (Lynch et al., 2016).

370 Products of Maillard reactions, e.g., melanoidins, are responsible for the change of
371 BSG's color (Wang et al., 2011). One of the factors significantly affecting the final color
372 change is reaction time, hence the residence time of material in the extruder. As proven by
373 other researchers (Haugaard et al., 1951), the depth of color increases with the square of time.
374 It is in line with the results of the presented study, which indicate that an increase of screw
375 speed during treatment in extruder increased BSG's lightness (see Table 1). As mentioned
376 above, also increasing throughput results in the shortening of residence time and exposition to
377 elevated temperature (Yeh et al., 1992). Nevertheless, both screw speed and increased
378 throughput may also show opposite effects, resulting in the enhancement of shear rate, hence
379 shear forces acting on the material, which increases the temperature of the material and results
380 in the darkening of material (Suprano et al., 2010). It can be seen that the increase in
381 throughput caused a slight lowering of the lightness of BSG samples.

382 Except for lightness also other color properties, such as chroma or hue (presented in
383 Table 1), are affected by the generation of melanoidins and resulting browning of BSG
384 (Echavarria et al., 2013a). According to CIELab color space, typical brown color is
385 characterized by a hue angle of ~50° (Berry, 1998). Therefore an increase of extrusion
386 temperature enhances the browning of BSG related to the generation of melanoidins



387 (Maillard, 1912). Morales and van Boekel (1998) demonstrated a positive correlation between
388 browning of casein/sugar solutions measured by spectrophotometer and chroma of generated
389 melanoidins. Later, Wu et al. (2011) confirmed these findings for the malt drying process,
390 during which chroma of malt was increasing with the content of melanoidins. Therefore, the
391 observed increase of chroma value should be considered as a potential indicator of
392 melanoidins' generation during extrusion grinding.

393 In the presented case, observed changes of color were not so strong because the
394 absence of moisture during Maillard reactions tends to minimize browning, which can be
395 noticed here, because of the relatively low moisture content of initial BSG (6.9 wt.%,
396 according to TGA analysis). Nevertheless, the presented data indicate that the color of filler,
397 which has a crucial impact on the appearance of the resulting composite (which is very
398 important for the recipients of final products), depends on the processing conditions. In most
399 cases, during the manufacturing of WPCs, filler pretreatment includes at least grinding aimed
400 at achieving the desired particle size, which impacts the mechanical performance of the
401 composite. Therefore, by adjustment of processing conditions, the desired color of the
402 resulting filler can be achieved. As a result, it could significantly reduce or even eliminate the
403 use of additional pigments or dyes, rarely composed only of natural compounds.

404

405 *3.3. Antioxidant activity*

406 For the manufacturing of WPCs, it can also be very interesting that melanoidins have
407 been reported to show noticeable antioxidant activity. Hence, their presence, in combination
408 with phenolic compounds (which can also be found in BSG), indicates that grinding may
409 provide additional, antioxidant properties to BSG, simultaneously enhancing the durability of
410 WPCs (Meneses et al., 2013). Such an effect was noted by other researchers for other natural
411 fillers showing antioxidant activity (Sarasini et al., 2018). Iver et al. (2015) noted that the



412 value of elongation at break was maintained at the same level after ten extrusion cycles for
413 low-density polyethylene composites filled with 4, 8, and 12 wt.% of grape waste, turmeric
414 waste and coffee grounds, respectively. Therefore, it is very interesting to investigate the
415 antioxidant properties of thermo-mechanically treated BSG, which could potentially enhance
416 the performance of WPCs. According to literature data, relatively high activity was observed
417 for melanoidins based on histidine, which, as mentioned above, which is a significant amino
418 acid of BSG (Yilmaz and Toledo, 2005). Based on these literature reports, further research
419 was aimed to examine the antioxidant properties of selected samples of extruded BSG. The
420 results of the performed tests are presented in Table 1.

421 Relatively high activity of the reference sample may be associated with the presence
422 of phenolic compounds in BSG, such as ferulic and *p*-coumaric acids (Mussatto et al., 2006).
423 It can be seen that performed modifications via extrusion grinding resulted in noticeable
424 enhancement of BSG's antioxidant activity. The highest inhibition effect was noted for
425 samples with the lowest lightness, which most likely contained the highest amount of
426 melanoidins. It can also be seen that despite relatively similar values of lightness, BSG
427 extruded at 120 and, especially at 180 °C showed higher antioxidant activity, suggesting a
428 more intensive generation of melanoidins. The increase of samples' chroma may confirm such
429 an assumption. A similar correlation between DPPH radical scavenging activity and a^* and
430 b^* , hence also chroma values for melanoidins was observed by Echavarría et al. (2013b).

431
432

433 *3.4. Fourier-transform infrared spectroscopy analysis*

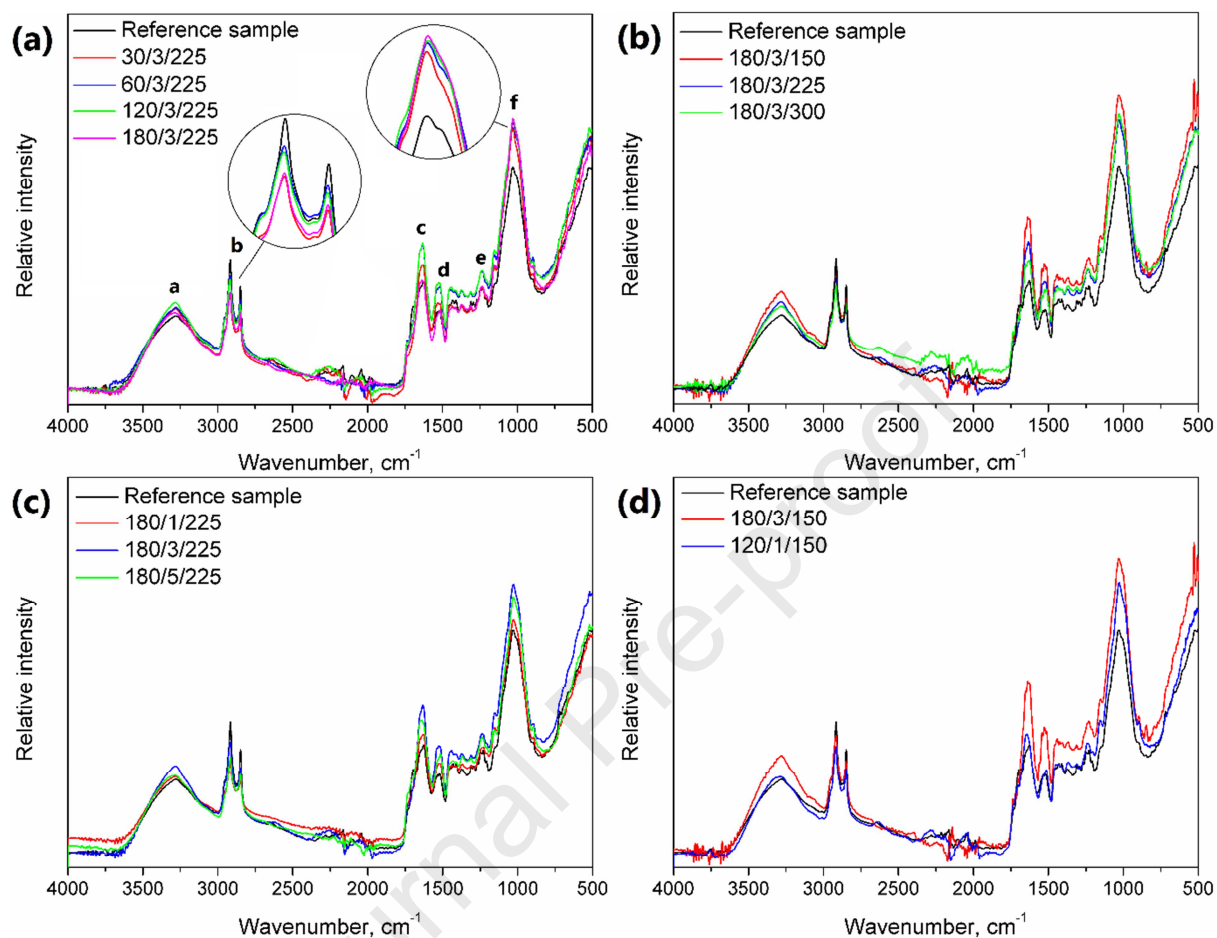
434 Fig. 4 shows the impact of the extrusion process and its parameters on the FTIR
435 spectra of BSG. Generally, analyzed materials showed spectra typical for lignocellulose
436 materials, such as wood flour, wheat bran, and others. All samples show typical signal (a)
437 around $3290-3300\text{ cm}^{-1}$, associated with the stretching vibrations of hydroxyl groups present



438 in the structure of polysaccharides, as well as the NH stretching vibrations related to the
439 presence of proteins in BSG (Mohsin et al., 2018). It can be seen that the intensity of this
440 signal is hardly affected by the extrusion of material. Fig. 4b indicated that the most
441 significant influence was noted for the screw speed, which directly affects the residence time
442 and level of shear forces acting on the material. The increase of these forces results in the
443 greater extent of materials decomposition and oxidation during the extrusion. In the range of
444 2850-2950 cm^{-1} , there are observed absorption bands (b) attributed to the symmetric and
445 asymmetric stretching vibrations of C-H bonds in methyl and methylene groups. The
446 extrusion treatment decreased the intensity of these bands, and it was more noticeable for
447 BSG modified at higher temperatures. Such an effect is associated with a greater extent of
448 polysaccharides decomposition and oxidation. Peaks (c) in the range of 1620-1700 cm^{-1} were
449 related to the stretching vibrations of unconjugated C=O and C=C bonds in polysaccharides,
450 but also to the amide I vibrations (stretching vibrations of C=O and C-N bonds in amide
451 groups) (Barth, 2007). Their intensity was increased by the extrusion treatment, which points
452 to oxidation of polysaccharides and the formation of melanoidins in Maillard reactions.
453 Signals (d) in the range of 1515-1550 cm^{-1} are due to amide II vibrations – the combination of
454 NH bending and CN stretching vibrations of amide groups. These signals, similar to (c), were
455 affected by extrusion treatment. The changes in processing parameters strongly influenced the
456 intensity of signals (c) and (d). Nevertheless, there was no straightforward impact because of
457 the contradictory effects of screw speed and throughput, related to the strength of shear forces
458 and residence time of material in the extruder barrel. Bands (e) and (f) in the range of 1220-
459 1240 and 1030 cm^{-1} are associated with stretching vibrations of C-O and C=O bonds present
460 in structures of polysaccharides (Hejna et al., 2020). The increase in their intensity confirms
461 the oxidation of polysaccharides during grinding. Slight shifts of positions of signals



462 associated with vibrations of carbon-oxygen are related to the chemical reactions occurring in
463 the system and resulting in new interactions.



466 **Figure 4.** FTIR spectra of extruded BSG depending on (a) temperature, (b) screw speed, and (c) throughput of
467 the process, as well as (d) spectra of samples with the lowest and the highest lightness.

468 Generally, presented FTIR spectra confirm the partial decomposition of
469 polysaccharides during extrusion treatment followed by their oxidation and occurring
470 Maillard reactions leading to the generation of melanoidins responsible for the color change.
471 In Fig. 4b, the impact of screw speed on the FTIR spectra is presented. It can be seen that
472 lower screw speed, hence longer residence time of material in the extruder, increased the
473 intensity of signals associated with the reactions mentioned above occurring in the material.
474 The most significant effect was noted for signal (f), which was related to the thermo-oxidation
475 of material during treatment. FTIR spectra were also influenced by process throughput, hence
476 the degree of fill, which affects the friction inside the barrel. Similar changes, compared to the

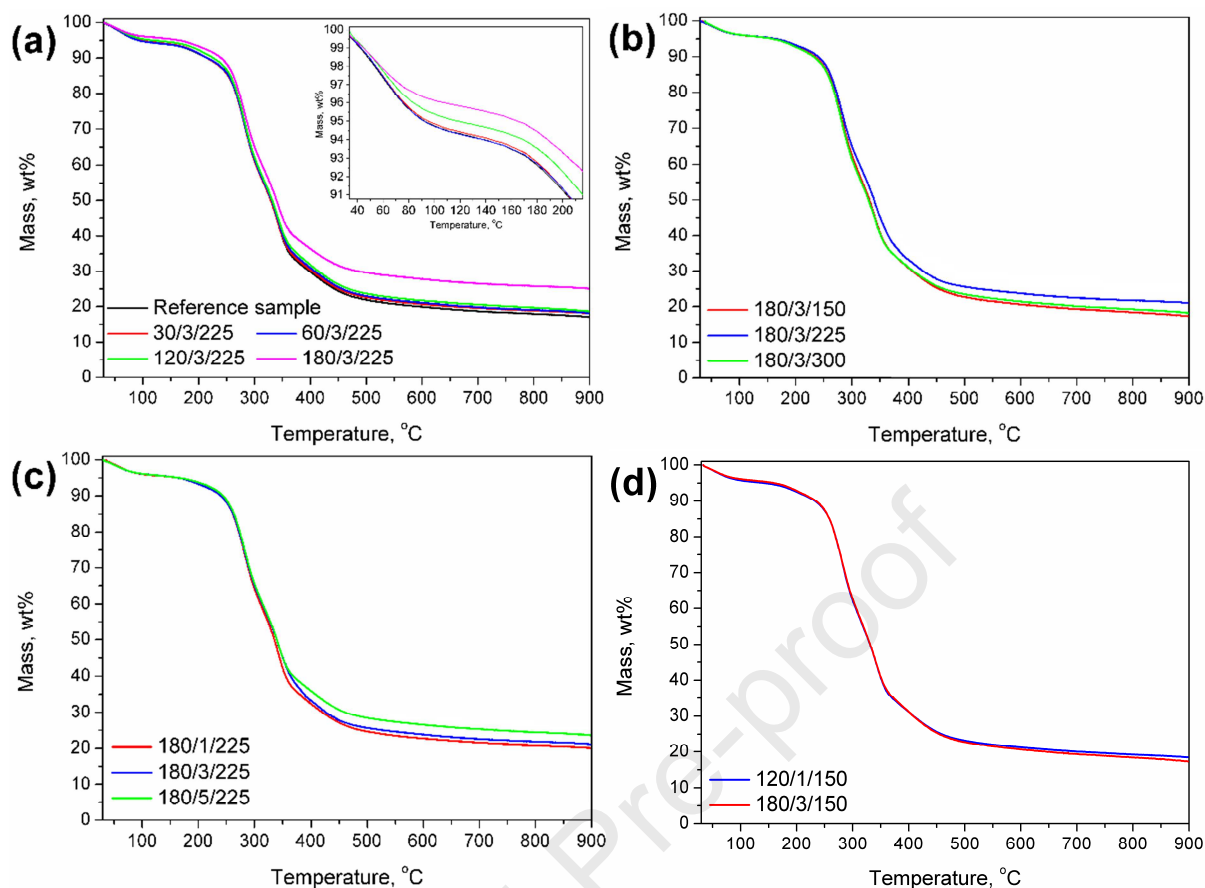
477 reference material, were noted. However, the effect was weaker than for the screw speed,
478 which suggests that residence time is a more significant factor than shear forces. Moreover, in
479 Fig. 4d there are shown spectra for the lightest (120/1/150) and for the darkest sample
480 (180/3/150), which indicates color changes were strictly associated with changes in the
481 chemical composition of BSG.

482 *3.5. Thermal stability*

483

484 The results of the thermogravimetric analysis performed for samples of extruded BSG
485 are presented in Fig. 5 and summarized in Table 2. It can be noticed that the extrusion process
486 caused some changes in the thermal stability of the material. The reduction of moisture
487 content was noted, which was measured as the magnitude of mass loss from 30 to 160 °C. It
488 probably also included the decomposition of some extractives. However, it is here presented
489 only for comparison purposes. The lowest content of moisture was noted for sample
490 180/3/225. It was mainly affected by the temperature of extrusion rather than throughput and
491 screw speed, which, as mentioned before, show opposite effects associated with shear forces
492 and residence time. The impact of extrusion temperature on the moisture content can be seen
493 in Fig. 5a. In general, the presence of moisture in the modified BSG samples was associated
494 with the hygroscopic character of natural fillers, which was confirmed by other researchers
495 (Almeida et al., 2018; George et al., 2001). However, the reduction of moisture content was
496 noted after treatment, which indicates changes in the polarity of the BSG surface.
497 Nevertheless, even samples extruded at higher temperatures contained over 4.5 wt.% of
498 moisture, which is still too much for the manufacturing of WPCs. Such values implicate the
499 drying of filler before the manufacturing of composites, which is commonly applied practice.





500

501

502 **Figure 5.** Thermogravimetric curves of extruded BSG depending on (a) temperature, (b) screw speed, and (c)
 503 throughput of the process, as well as (d) spectra of samples with the lowest and the highest lightness.

504 Generally, extrusion of BSG and increase of extrusion temperature enhanced BSG's
 505 thermal stability, which can be expressed by the rise of temperature associated with 5 wt.%
 506 mass loss during analysis ($T_{5\%}$). Such an effect can be associated with the reduction in the
 507 content of low molecular weight compounds, which may take part in Maillard reactions or can
 508 be degraded during processing at higher temperatures. Most of the weight loss of BSG occurs
 509 between 160 and 500 °C. In this range, there can be noticed two peaks on DTG curves, which
 510 are related to the decomposition of hemicelluloses and cellulose, ~281 and ~341 °C,
 511 respectively, which is in line with the results presented by other researchers (Vanreppelen et
 512 al., 2014). Independently of extrusion parameters, char yield at a temperature of 900 °C was
 513 very similar in the range of 18-19 wt.%, which is typical for BSG (Mahmood et al., 2013).

514 **Table 2.** Results of thermogravimetric analysis of extruded BSG samples.

Temperature, °C	Throughput, kg/h	Screw speed, rpm	Moisture content, wt. %	T _{1%} , °C	T _{5%} , °C	T _{50%} , °C	T _{max1} , °C	T _{max2} , °C	
Reference sample			6.90	43.7	91.7	332.6	281.1	346.8	
30	3	225	6.05	43.0	95.4	329.1	281.2	341.4	
60			6.20	42.8	92.3	329.9	281.3	342.0	
120			5.50	44.6	117.1	332.1	280.7	342.3	
180			4.65	45.1	159.3	340.0	282.0	340.2	
			4.70	45.5	162.9	332.4	279.5	341.3	
180	3	225	4.65	45.1	159.3	340.0	282.0	340.2	
		300	4.85	46.8	152.7	332.3	281.0	342.0	
		1	4.85	46.1	157.2	335.0	281.4	344.1	
180	3	225	4.65	45.1	159.3	340.0	282.0	340.2	
			5	4.65	45.2	162.2	340.0	281.2	341.8
120			1	150	5.10	44.7	139.2	332.3	280.7
180	3	150	4.70	45.5	162.9	332.4	279.5	341.3	

515

516

517 *3.6. Energy consumption*

518

519

520

521

522

523

524

525

526

527

528

529

From the industrial point of view, an essential aspect of all processes included in the production cycle is energy consumption, which has a direct impact on the cost-efficiency of production. Grinding processes are considered as very energy-intensive. Therefore their investigations and optimization are significant (Li et al., 2012). On the other hand, twin-screw extrusion is considered a mechanical treatment method characterized by low energy demand (Rol et al., 2017). In Table 3, there are presented values of SME calculated according to equation (20) presented in 2.3. Measurements section. It can be seen that the amount of energy required to process BSG generally decreases with higher screw speed, which is directly associated with the residence time of material in the extruder barrel (Kelly et al., 2006). For higher temperatures, this effect was not so evident and strong, due to the above mentioned opposite effects of screw speed.

530 **Table 3.** Values of specific mechanical energy required for extrusion grinding of BSG under various conditions.

Temperature, °C	Throughput, kg/h	Screw speed, rpm	Motor load, %	SME, kWh/kg
30	1	75	55.5	0.872
		150	21.0	0.660
		225	13.5	0.636
	3	150	72.0	0.754
		225	41.5	0.652
		300	27.0	0.565
	5	225	76.5	0.721
		300	52.5	0.662
		375	37.0	0.581
60	1	75	42.0	0.660
		150	18.0	0.565
		225	11.5	0.542
	3	150	59.5	0.623
		225	35.0	0.550
		300	24.0	0.503
	5	225	64.0	0.603
		300	45.0	0.565
		375	34.5	0.542
120	1	75	23.5	0.369
		150	11.5	0.361
		225	8.5	0.400
	3	150	36.5	0.382
		225	19.5	0.306
		300	14.5	0.304
	5	225	34.5	0.325
		300	23.5	0.295
		375	19.5	0.306
180	1	75	26.0	0.408
		150	12.0	0.377
		225	8.5	0.400
	3	150	38.0	0.398
		225	19.0	0.298
		300	14.0	0.293
	5	225	29.5	0.278
		300	20.5	0.258
		375	17.0	0.267

531
 532 At 30 and 60 °C, SME was slightly increasing with throughput, which was associated
 533 with an increase in friction between the extruder barrel and processed material (Rasid and

534 Wood, 2003). At higher temperatures, friction was probably reduced due to the presence of a
 535 slight amount of water generated during Maillard reactions. It cannot be neglected that for
 536 materials processed with higher temperature values, i.e., 120 and 180 °C, low molecular
 537 weight products migrating from organic particles as well as decomposition products provide
 538 to the reduction of internal friction, which results in lowered SME values during extrusion.

539 **Table 4.** Dependence of SME on various extrusion parameters.

Dependence of SME vs								
Screw speed (R)			Temperature (T)			Throughput (Y)		
T, °C	Y, kg/h	R ²	Y, kg/h	R, rpm	R ²	T, °C	R, rpm	R ²
30	1	0.825	1	75	0.788	30	225	0.865
30	3	0.998	1	150	0.828	60	225	0.847
30	5	0.992	1	225	0.848	120	225	0.569
60	1	0.890	3	150	0.830	180	225	0.869
60	3	0.985	3	225	0.876			
60	5	0.980	3	300	0.886			
120	1	0.566	5	225	0.919			
120	3	0.769	5	300	0.912			
120	5	0.392	5	375	0.916			
180	1	0.062						
180	3	0.786						
180	5	0.302						

540
 541 Table 4 presents the values of correlation coefficients (R^2) for dependences of SME
 542 vs. screw speed, temperature, and throughput. It can be seen that the best correlation can be
 543 observed for the temperature dependence of SME, which is in line with data presented by
 544 other researchers (Abeykoon et al., 2009, 2014). Lower values of R^2 , observed mainly for the
 545 dependence of SME vs. screw speed at higher temperatures, are associated with very similar
 546 values of SME (see Table 3).

548 4. Conclusions

549 The structure and properties of brewers' spent grain subjected to extrusion grinding
 550 were investigated in order to determine its potential for application as filler for wood polymer

551 composites. BSG was extruded in various conditions to analyze the impact of process
552 temperature, throughput, and screw speed, which affect the magnitude of shear forces acting
553 on material and material residence time in the extruder barrel. The most significant influence
554 was observed for temperature since both throughput and screw speed show opposite effects.

555 In the case of particle size, very important for the manufacturing of WPCs, the rise of
556 temperature led to more than two-fold size reduction, from 466 and 557 μm for 30 and 60 $^{\circ}\text{C}$
557 to 203 and 138 μm , respectively for 120 and 180 $^{\circ}\text{C}$. In the case of lower temperatures,
558 unfavorable granulation of BSG was observed, which on the other side could be desired, i.e.,
559 in the food industry. The influence of screw speed, and especially throughput, was not so
560 significant.

561 Together with changes in chemical structure, particle size noticeably affected the color
562 of the resulting material, which is crucial for the end-products users. The highest values of
563 lightness, exceeding 55, were noted for samples extruded at 120 $^{\circ}\text{C}$, so this parameter was
564 increased by almost 15% despite occurring browning reactions (whose intensity was moderate
565 at this temperature). Further rise of temperature resulted in the intensification of Maillard
566 browning reactions and significant changes in BSG's color. These changes were confirmed by
567 FTIR analysis and rising antioxidant activity of material, which was associated with the
568 presence of melanoidins, generated during processing. After extrusion at 180 $^{\circ}\text{C}$, antioxidant
569 activity was even doubled compared to the reference sample and 35% higher than after
570 processing at 120 $^{\circ}\text{C}$.

571 Higher processing temperatures also resulted in the enhancement of the thermal
572 stability of BSG samples, which was related to the reduction of moisture content and possible
573 partial decomposition and evaporation of its products. This phenomenon also favorably
574 affected the specific mechanical energy required for extrusion of BSG, by reduction of
575 internal friction inside the extruder barrel. For the temperatures of 120 and 180 $^{\circ}\text{C}$, SME was



576 in the range of 0.25-0.41 kWh/kg, comparing to 0.50-0.66 for 60 °C, and 0.56-0.87 for 30 °C.
577 Such an effect may noticeably affect the economic aspect of BSG extrusion.

578 Generally, it was proven that extrusion of BSG might be considered an effective
579 method for the preparation of fillers for WPC manufacturing, whose properties may be
580 engineered by proper adjustment of extrusion parameters. Nevertheless, to enhance the
581 industrial potential of the investigated process, the following issues should be addressed:

- 582 • emissions of volatile organic compounds should be analyzed, both in qualitative and
583 quantitative terms, to determine the safety of the process considering health aspects,
- 584 • total energy use, related not only to the specific mechanical energy needed for screws
585 rotation but also to heating the extrusion barrel, should be determined for different
586 parameters of the process so that the economic calculations could be made,
- 587 • for similar reasons, the amount of water used during extrusion should be calculated and
588 included in the economic calculations,
- 589 • the influence of BSG melanoidins generated during treatment on the resistance of various
590 polymer matrices towards oxidation should be evaluated,
- 591 • the possibility of incorporation of additional modifiers enhancing the compatibility of
592 modified BSG with polymer matrices should be evaluated.

593 These issues should be investigated in further works related to the thermo-mechanical
594 treatment of brewers' spent grain via the extrusion process.

595 Moreover, the presented results indicate that except for the application in the
596 manufacturing of polymer composites, modified brewers' spent grain may also be applied,
597 e.g., as a functional food ingredient. According to the characteristics of the mashing process
598 (source of BSG) and literature data, BSG contains very significant amounts of dietary fiber,
599 which is very beneficial from the nutritional point of view. The increase of melanoidins
600 content resulting from the extrusion treatment significantly increases the antioxidant activity

601 of BSG. Therefore, it could be used as a substitute for conventional flour, simultaneously
602 reducing the caloric value of food products and enhancing their shelf life.

603

604 **Acknowledgments**

605 This work was supported by the National Science Centre (NCN, Poland) in the frame
606 of SONATINA 2 project 2018/28/C/ST8/00187 - *Structure and properties of lignocellulosic*
607 *fillers modified in situ during reactive extrusion.*

608

609 **Conflict of interest**

610 On behalf of all authors, the corresponding author states that there is no conflict of
611 interest.

612

613 **References**

614 Abeykoon, C., Kelly, A.L., Brown, E.C., Vera-Sorroche, J., Coates, P.D., Harkin-Jones,
615 E., Howell, K.B., Deng, J., Li, K., Price, M., 2014. Investigation of the process energy
616 demand in polymer extrusion: A brief review and an experimental study. *Appl. Energ.*
617 136, 726–737. <https://doi.org/10.1016/j.apenergy.2014.09.024>

618 Abeykoon, C., McAfee, M., Thompson, S., Li, K., Kelly, A.L., Brown, E.C., 2009.
619 Investigation of torque fluctuations in extrusion through monitoring of motor variables, in:
620 Proceedings of 26th PPS annual Europe/Africa regional meeting, Larnaca, Cyprus, paper
621 no: 22-O.

622 Adobe Systems Incorporated, 2005. Adobe RGB (1998) Color Image Encoding, Version
623 2005-05. <https://www.adobe.com/digitalimag/pdfs/AdobeRGB1998.pdf> (accessed 18
624 April 2019).



625 Ahmed, J., Al-Attar, H., Arfat, Y.A., 2016. Effect of particle size on compositional,
626 functional, pasting and rheological properties of commercial water chestnut flour. *Food*
627 *Hydrocolloid.* 52, 888–895. <https://doi.org/10.1016/j.foodhyd.2015.08.028>

628 Ahmed, J., Al-Foudari, M., Al-Salman, F., Almusallam, A.S., 2014. Effect of particle size
629 and temperature on rheological, thermal, and structural properties of pumpkin flour
630 dispersion. *J. Food Eng.* 124, 43–53. <https://doi.org/10.1016/j.jfoodeng.2013.09.030>

631 Ahmed, J., Al-Jassar, S., Thomas, L., 2015. A comparison in rheological, thermal, and
632 structural properties between Indian Basmati and Egyptian Giza rice flour dispersions as
633 influenced by particle size. *Food Hydrocolloid.* 48, 72–83.
634 <https://doi.org/10.1016/j.foodhyd.2015.02.012>

635 Almeida, G., Remond, R., Perre, P., 2018. Hygroscopic behaviour of lignocellulosic
636 materials: Dataset at oscillating relative humidity variations. *J. Build. Eng.* 19, 320–333.
637 <https://doi.org/10.1016/j.job.2018.05.005>

638 Altomare, R.E., Ghossi, P., 1986. An analysis of residence time distribution patterns in a
639 twin screw cooking extruder. *Biotechnol. Progr.* 2 (3), 157–163.
640 <https://doi.org/10.1002/btpr.5420020310>

641 Barth, A., 2007. Infrared spectroscopy of proteins. *BBA-Bioenergetics* 1767 (9), 1073–
642 1101. <https://doi.org/10.1016/j.bbabi.2007.06.004>

643 Berry, B.W., 1998. Cooked color in high pH beef patties as related to fat content and
644 cooking from the frozen or thawed state. *J. Food Sci.* 63 (5), 797–800.
645 <https://doi.org/10.1111/j.1365-2621.1998.tb17903.x>

646 Berthet, M.A., Angellier-Coussy, H., Machado, D., Hilliou, L., Staebler, A., Vicente, A.,
647 Gontard, N., 2015. Exploring the potentialities of using lignocellulosic fibres derived from
648 three food by-products as constituents of biocomposites for food packaging. *Ind. Crop.*
649 *Prod.* 69, 110–122. <https://doi.org/10.1016/j.indcrop.2015.01.028>

650 Bociaga, E., Trzaskalska, M., 2016. Influence of polymer processing parameters and
651 coloring agents on gloss and color of acrylonitrile-butadiene-styrene terpolymer moldings.
652 *Polimery* 61, 544–550. <https://doi.org/10.14314/polimery.2016.544>

653 Bolade, M.K., Adeyemi, I.A., Ogunsua, A.O., 2009. Influence of particle size fractions on
654 the physicochemical properties of maize flour and textural characteristics of a maize-
655 based nonfermented food gel. *Int. J. Food Sci. Tech.* 44 (3), 646–655.
656 <https://doi.org/10.1111/j.1365-2621.2008.01903.x>

657 Brand-Williams, W., Cuvelier, M.E., Berset, C., 1995. Use of a free radical method to
658 evaluate antioxidant activity. *LWT-Food Sci. Technol.* 28 (1), 25–30.
659 [https://doi.org/10.1016/S0023-6438\(95\)80008-5](https://doi.org/10.1016/S0023-6438(95)80008-5)

660 Bridgeman, T.G., Darvell, L.I., Jones, J.M., Williams, P.T., Fahmi, R., Bridgwater, A.V.,
661 Barraclough, T., Shield, I., Yates, N., Thain, S.C., Donnison, I.S., 2007. Influence of
662 particle size on the analytical and chemical properties of two energy crops. *Fuel* 86 (1-2),
663 60–72. <https://doi.org/10.1016/j.fuel.2006.06.022>

664 Chen, Q., Koh, H.K., Park, J.B., 1999. Color evaluation of red pepper powder. *T. ASAE*
665 42 (3), 749–752.

666 Cunha, M., Berthet, M.A., Pereira, R., Covas, J.A., Vicente, A.A., Hilliou, L., 2014.
667 Development of polyhydroxyalkanoate/beer spent grain fibers composites for film
668 blowing applications. *Polym. Compos.* 36 (10), 1859–1865.
669 <https://doi.org/10.1002/pc.23093>

670 Dhanalakshmi, K., Ghosal, S., Bhattacharya, S., 2011. Agglomeration of food powder and
671 applications. *Crit. Rev. Food Sci.* 51 (5), 432–441.
672 <https://doi.org/10.1080/10408391003646270>



673 Duque, A., Manzanares, P., Ballesteros, M., 2017. Extrusion as a pretreatment for
674 lignocellulosic biomass: Fundamentals and applications. *Renew. Energ.* 114, 1427–1441.
675 <https://doi.org/10.1016/j.renene.2017.06.050>

676 Echavarría, A., Pagán, J., Ibarz, A., 2013a. Kinetics of color development of melanoidins
677 formed from fructose/amino acid model system. *Food Sci. Technol. Int.* 20 (2), 119–126.
678 <https://doi.org/10.1177/1082013213476071>

679 Echavarría, A., Pagan, J., Ibarz, A., 2013b. Optimization of Maillard reaction products
680 isolated from sugar-amino acid model system and their antioxidant activity. *Afinidad* 70,
681 86–92.

682 Formela, K., Cysewska, M., Haponiuk, J., 2014. The influence of screw configuration and
683 screw speed of co-rotating twin screw extruder on the properties of products obtained by
684 thermomechanical reclaiming of ground tire rubber. *Polimery* 59 (2), 170–177.
685 <https://doi.org/10.14314/polimery.2014.165>

686 Formela, K., Hejna, A., Zedler, Ł., Przybysz, M., Ryl, J., Saeb, M.R., Piszczyk, Ł., 2017.
687 Structural, thermal and physico-mechanical properties of polyurethane/brewers' spent
688 grain composite foams modified with ground tire rubber. *Ind. Crop. Prod.* 108, 844–852.
689 <https://doi.org/10.1016/j.indcrop.2017.07.047>

690 Fu, S.Y., Feng, X.Q., Lauke, B., Mai, Y.W., 2008. Effects of particle size, particle/matrix
691 interface adhesion and particle loading on mechanical properties of particulate–polymer
692 composites. *Compos. Part B-Eng.* 39 (6), 933–961.
693 <https://doi.org/10.1016/j.compositesb.2008.01.002>

694 George, J., Sreekala, M.S., Thomas, S., 2001. A review on interface modification and
695 characterization of natural fiber reinforced plastic composites. *Polym. Eng. Sci.* 41 (9),
696 1471–1485. <https://doi.org/10.1002/pen.10846>



697 Haugaard, G., Tumerman, L., Silvestri, H., 1951. A Study on the Reaction of Aldoses and
698 Amino Acids. *J. Am. Chem. Soc.* 73, 4594–4600. <https://doi.org/10.1021/ja01154a028>
699 Hejna, A., Formela, K., 2019. Sposób suszenia i rozdrabniania młóta browarnianego.
700 Polish patent application P.430449.
701 Hejna, A., Formela, K., Reza Saeb, M., 2015. Processing, mechanical and thermal
702 behavior assessments of polycaprolactone/agricultural wastes biocomposites. *Ind. Crop.*
703 *Prod.* 76, 725–733. <https://doi.org/10.1016/j.indcrop.2015.07.049>
704 Hejna, A., Haponiuk, J., Piszczyk, Ł., Klein, M., Formela, K., 2017. Performance
705 properties of rigid polyurethane-polyisocyanurate/brewers' spent grain foamed composites
706 as function of isocyanate index. *e-Polymers* 17 (5), 427–437.
707 <https://doi.org/10.1515/epoly-2017-0012>
708 Hejna, A., Sulyman, M., Przybysz, M., Saeb, M.R., Klein, M., Formela, K., 2020. On the
709 correlation of lignocellulosic filler composition with the performance properties of poly(ϵ -
710 caprolactone) based biocomposites. *Waste Biomass Valori.* 11, 1467–1479.
711 <https://doi.org/10.1007/s12649-018-0485-5>
712 Horvath, Z.H., Halasz-Fekete, M., 2005. Instrumental colour measurement of paprika
713 grist. *Ann. Fac. Eng. Hunedoara* 3, 101–106.
714 Hunt, R.W.G., 2004. *The Reproduction of Colour* (6th ed.). Wiley, Chichester, UK.
715 International Commission on Illumination, 1978. Recommendations on uniform color
716 spaces, color-difference equations, psychometric color terms. Bureau central de la C.I.E.,
717 Paris, France.
718 Iyer, K.A., Zhang, L., Torkelson, J.M., 2015. Direct use of natural antioxidant-rich agro-
719 wastes as thermal stabilizer for polymer: Processing and recycling. *ACS Sustain. Chem.*
720 *Eng.* 4 (3), 881–889. <https://doi.org/10.1021/acssuschemeng.5b00945>



721 Kao, S.V., Allison, G.R., 1984. Residence time distribution in a twin screw extruder.
722 Polym. Eng. Sci. 24 (9), 645–651. <https://doi.org/10.1002/pen.760240906>

723 Kargarzadeh, H., Huang, J., Lin, N., Ahmad, I., Mariano, M., Dufresne, A., Thomas, S.,
724 Gałęski, A., 2018. Recent developments in nanocellulose-based biodegradable polymers,
725 thermoplastic polymers, and porous nanocomposites. Prog. Polym. Sci. 87, 197–227.
726 <https://doi.org/10.1016/j.progpolymsci.2018.07.008>

727 Kargarzadeh, H., Mariano, M., Huang, J., Lin, N., Ahmad, I., Dufresne, A., Thomas, S.,
728 2017. Recent developments on nanocellulose reinforced polymer nanocomposites: A
729 review. Polymer 132, 368–393. <https://doi.org/10.1016/j.polymer.2017.09.043>

730 Kelly, A.L., Brown, E.C., Coates, P.D., 2006. The effect of screw geometry on melt
731 temperature profile in single screw extrusion. Polym. Eng. Sci. 46 (12), 1706–1714.
732 <https://doi.org/10.1002/pen.20657>

733 Kim, J.M., Shin, M., 2014. Effects of particle size distributions of rice flour on the quality
734 of gluten-free rice cupcakes. LWT-Food Sci. Tech. 59 (1), 526–532.
735 <https://doi.org/10.1016/j.lwt.2014.04.042>

736 Leonard, W., Zhang, P., Ying, D., Fang, Z., 2019. Application of extrusion technology in
737 plant food processing by-products: An overview. Compr. Rev. Food Sci. F. 19 (1), 218–
738 246. <https://doi.org/10.1111/1541-4337.12514>

739 Li, W., Winter, M., Kara, S., Herrmann, C., 2012. Eco-efficiency of manufacturing
740 processes: A grinding case. CIRP Ann. 61 (1), 59–62.
741 <https://doi.org/10.1016/j.cirp.2012.03.029>

742 Liu, K., 2009. Effects of particle size distribution, compositional and color properties of
743 ground corn on quality of distillers dried grains with solubles (DDGS). Bioresource
744 Technol. 100 (19), 4433–4440. <https://doi.org/10.1016/j.biortech.2009.02.067>



745 López, F., Valiente, J.M., Baldrich, R., Vanrell, M., 2005. Fast Surface Grading Using
746 Color Statistics in the CIE Lab Space, in: Marques, J.S., Pérez de la Blanca, N., Pina, P.
747 (Eds.), Pattern Recognition and Image Analysis. IbPRIA 2005. Springer, Berlin,
748 Heidelberg, pp. 666-673. https://doi.org/10.1007/11492542_81

749 Lynch, K.M., Steffen, E.J., Arendt, E.K., 2016. Brewers' spent grain: a review with an
750 emphasis on food and health. *J. I. Brewing* 122 (4), 553–568.
751 <https://doi.org/10.1002/jib.363>

752 Mahmood, A.S.N., Brammer, J.G., Hornung, A., Steele, A., Poulston, S., 2013. The
753 intermediate pyrolysis and catalytic steam reforming of Brewers spent grain. *J. Anal.*
754 *Appl. Pyrol.* 103, 328–342. <https://doi.org/10.1016/j.jaap.2012.09.009>

755 Maillard, L.C., 1912. Action des acides amines sur les sucres; formation de melanoidines
756 par voie méthodique. *Compt. Rend.* 154, 66-68.

757 Market Research Store, 2018. Global Wood Plastic Composites (Wpc) Market Report
758 2018 - Industry Analysis, Size, Share, Trends, Segment and Forecasts to 2025.
759 [https://www.marketresearchstore.com/report/global-wood-plastic-composites-wpc-](https://www.marketresearchstore.com/report/global-wood-plastic-composites-wpc-market-report-2018-303554)
760 [market-report-2018-303554](https://www.marketresearchstore.com/report/global-wood-plastic-composites-wpc-market-report-2018-303554) (accessed 18 April 2019).

761 Martins, S.I.F., Jongen, W.M., van Boekel, M.A.J., 2000. A review of Maillard reaction in
762 food and implications to kinetic modelling. *Trends Food Sci. Tech.* 11 (9-10), 364–373.
763 [https://doi.org/10.1016/S0924-2244\(01\)00022-X](https://doi.org/10.1016/S0924-2244(01)00022-X)

764 Meneses, N.G., Martins, S., Teixeira, J.A., Mussatto, S.I., 2013. Influence of extraction
765 solvents on the recovery of antioxidant phenolic compounds from brewer's spent grains.
766 *Sep. Purif. Technol.* 108, 152–158. <https://doi.org/10.1016/j.seppur.2013.02.015>

767 Mohsin, G.F., Schmitt, F.J., Kanzler, C., Dirk Epping, J., Flemig, S., Hornemann, A.,
768 2018. Structural characterization of melanoidin formed from d -glucose and l -alanine at



769 different temperatures applying FTIR, NMR, EPR, and MALDI-ToF-MS. *Food Chem.*
770 245, 761–767. <https://doi.org/10.1016/j.foodchem.2017.11.115>

771 Moraczewski, K., Stepczyńska, M., Malinowski, R., Karasiewicz, T., Jagodziński, B.,
772 Rytlewski, P., 2019. The Effect of Accelerated Aging on Polylactide Containing Plant
773 Extracts. *Polymers* 11(4), 575. <https://doi.org/10.3390/polym11040575>

774 Morales, F.J., van Boekel, M.A.J.S., 1998. A Study on Advanced Maillard Reaction in
775 Heated Casein/Sugar Solutions: Colour Formation. *Int. Dairy J.* 8 (10-11), 907–915.

776 Mussatto, S.I., Dragone, G., Roberto, I.C., 2006. Brewer's spent grain: generation,
777 characteristics and potential applications. *J. Cereal Sci.* 43, 1-14.
778 <https://doi.org/10.1016/j.jcs.2005.06.001>

779 Offiah, V., Kontogiorgos, V., Falade, K.O., 2018. Extrusion processing of raw food
780 materials and by-products: A review. *Crit. Rev. Food Sci.* 59 (18), 2979–2998.
781 <https://doi.org/10.1080/10408398.2018.1480007>

782 Ott, R.L., 1964. Mechanism of the mechanical degradation of cellulose. *J. Polym. Sci.*
783 Part A 2 (2), 973–982. <https://doi.org/10.1002/pol.1964.100020232>

784 Pastoriza, S., Rufián-Henares, J.A., 2014. Contribution of melanoidins to the antioxidant
785 capacity of the Spanish diet. *Food Chem.* 164, 438–445.
786 <https://doi.org/10.1016/j.foodchem.2014.04.118>

787 Rasid, R., Wood, A.K., 2003. Effect of process variables on melt temperature profiles in
788 extrusion process using single screw plastics extruder. *Plast. Rubber Compos.* 32 (5),
789 187–192. <https://doi.org/10.1179/146580103225002731>

790 Revert, A., Reig, M., Seguí, V.J., Boronat, T., Fombuena, V., Balart, R., 2015. Upgrading
791 brewer's spent grain as functional filler in polypropylene matrix. *Polym. Compos.* 38 (1),
792 40–47. <https://doi.org/10.1002/pc.23558>



793 Rivero-Pérez, M.D., Pérez-Magariño, S., González-San José, M.L., 2002. Role of
794 melanoidins in sweet wines. *Anal. Chim. Acta* 458 (1), 169–175.
795 [https://doi.org/10.1016/s0003-2670\(01\)01591-4](https://doi.org/10.1016/s0003-2670(01)01591-4)

796 Rol, F., Karakashov, B., Nechyporchuk, O., Terrien, M., Meyer, V., Dufresne, A.,
797 Belgacem, M.N., Bras, J., 2017. Pilot-Scale Twin Screw Extrusion and Chemical
798 Pretreatment as an Energy-Efficient Method for the Production of Nanofibrillated
799 Cellulose at High Solid Content. *ACS Sustain. Chem. Eng.* 5 (8), 6524–6531.
800 <https://doi.org/10.1021/acssuschemeng.7b00630>

801 Rufián-Henares, J.A., Morales, F.J., 2007. Functional properties of melanoidins: In vitro
802 antioxidant, antimicrobial and antihypertensive activities. *Food Res. Int.* 40 (8), 995–
803 1002. <https://doi.org/10.1016/j.foodres.2007.05.002>

804 Sahputra, I.H., Alexiadis, A., Adams, M.J., 2019. Effects of moisture on the mechanical
805 properties of microcrystalline cellulose and the mobility of the water molecules as studied
806 by the hybrid molecular mechanics-molecular dynamics simulation method. *J. Polym. Sci.*
807 *Pol. Phys.* 57 (8), 454–464. <https://doi.org/10.1002/polb.24801>

808 Sarasini, F., Tirillò, J., Zuorro, A., Maffei, G., Lavecchia, R., Puglia, D., Dominici, F.,
809 Luzi, F., Valente, T., Torre, L., 2018. Recycling coffee silverskin in sustainable
810 composites based on a poly(butylene adipate-co-terephthalate)/poly(3-hydroxybutyrate-
811 co-3-hydroxyvalerate) matrix. *Ind. Crop. Prod.* 118, 311–320.
812 <https://doi.org/10.1016/j.indcrop.2018.03.070>

813 Silva, G.G.D., Guilbert, S., Rouau, X., 2011. Successive centrifugal grinding and sieving
814 of wheat straw. *Powder Technol.* 208 (2), 266–270.
815 <https://doi.org/10.1016/j.powtec.2010.08.015>

816 Sun, C., Liu, R., Ni, K., Wu, T., Luo, X., Liang, B., Zhang, M., 2016. Reduction of
817 particle size based on superfine grinding: Effects on structure, rheological and gelling



818 properties of whey protein concentrate. *J. Food Eng.* 186, 69–76.
819 <https://doi.org/10.1016/j.jfoodeng.2016.03.002>

820 Suparno, M., Dolan, K.D., Ng, P.K.W., Steffe, J.F., 2010. Average shear rate in a twin-
821 screw extruder as a function of degree of fill, flow behavior index, screw speed and screw
822 configuration. *J. Food Process Eng.* 34 (4), 961–982. [https://doi.org/10.1111/j.1745-](https://doi.org/10.1111/j.1745-4530.2009.00381.x)
823 [4530.2009.00381.x](https://doi.org/10.1111/j.1745-4530.2009.00381.x)

824 The Brewers of Europe, 2018. Beer statistics, 2018 edition.
825 [https://brewersofeurope.org/uploads/mycms-files/documents/publications/2018/EU-beer-](https://brewersofeurope.org/uploads/mycms-files/documents/publications/2018/EU-beer-statistics-2018-web.pdf)
826 [statistics-2018-web.pdf](https://brewersofeurope.org/uploads/mycms-files/documents/publications/2018/EU-beer-statistics-2018-web.pdf) (accessed 18 April 2019).

827 Wang, H.Y., Qian, H., Yao, W.R., 2011. Melanoidins produced by the Maillard reaction:
828 Structure and biological activity. *Food Chem.* 128 (3), 573–584.
829 <https://doi.org/10.1016/j.foodchem.2011.03.075>

830 Vanreppelen, K., Vanderheyden, S., Kuppens, T., Schreurs, S., Yperman, J., Carleer, R.,
831 2014. Activated carbon from pyrolysis of brewer's spent grain: Production and adsorption
832 properties. *Waste Manage. Res.* 32 (7), 634–645.
833 <https://doi.org/10.1177/0734242X14538306>

834 Waters, D.M., Jacob, F., Titze, J., Arendt, E.K., Zannini, E., 2012. Fibre, protein and
835 mineral fortification of wheat bread through milled and fermented brewer's spent grain
836 enrichment. *Eur. Food Res. Technol.* 235 (5), 767–778. [https://doi.org/10.1007/s00217-](https://doi.org/10.1007/s00217-012-1805-9)
837 [012-1805-9](https://doi.org/10.1007/s00217-012-1805-9)

838 Villamiel, M., del Castillo, M.D., Corzo, N., 2006. 4. Browning Reactions, in: Hui, Y.H.,
839 Nip, W.K., Nollet, L.M.L., Paliyath, G., Simpson, B.K. (Eds.), *Food biochemistry and*
840 *food processing*. Wiley-Blackwell, New York, pp. 71–100.
841 <https://doi.org/10.1002/9781118308035.ch4>



842 Wu, H.B., Yun, J.M., Li, Y., Han, P., 2011. Relationship between malt chroma and
843 melanoidin at different drying conditions. *Journal of Gansu Agricultural University* 45,
844 130–133.

845 Yeh, A.I., Hwang, S.J., Guo, J.J., 1992. Effects of screw speed and feed rate on residence
846 time distribution and axial mixing of wheat flour in a twin-screw extruder. *J. Food Eng.*
847 17 (1), 1–13. [https://doi.org/10.1016/0260-8774\(92\)90061-A](https://doi.org/10.1016/0260-8774(92)90061-A)

848 Yilmaz, Y., Toledo, R., 2005. Antioxidant activity of water-soluble Maillard reaction
849 products. *Food Chem.* 93 (2), 273–278. <https://doi.org/10.1016/j.foodchem.2004.09.043>

850 Zajchowski, S., Ryszkowska, J., 2009. Kompozyty polimerowo-drzewne –
851 charakterystyka ogólna oraz ich otrzymywanie z materiałów odpadowych. *Polimery* 54
852 (10), 674-682.

853 Zedler, Ł., Colom, X., Cañavate, J., Saeb, M.R., Haponiuk, J.T., Formela, K., 2020.
854 Investigating the impact of curing system on structure-property relationship of natural
855 rubber modified with brewery by-product and ground tire rubber. *Polymers* 12, 545.
856 <https://doi.org/10.3390/polym12030545>

857 Zedler, Ł., Colom, X., Saeb, M.R., Formela, K., 2018. Preparation and characterization of
858 natural rubber composites highly filled with brewers' spent grain/ground tire rubber
859 hybrid reinforcement. *Compos. Part B-Eng.* 145, 182–188.
860 <https://doi.org/10.1016/j.compositesb.2018.03.024>

- Upcycling of brewers' spent grain (BSG) by treatment of twin-screw extruder
- Evaluation of temperature, throughput and rotational speed on properties of BSG
- Adjustment of extrusion parameters leads to desired appearance and properties of BSG
- Treated BSG was characterized by higher thermal stability and antioxidant activity
- Extrusion of BSG allows extend its applications in wood polymer composites technology

Journal Pre-proof